EIGENVALUE BUCKLING ANALYSIS OF FUNCTIONALLY GRADED GRAPHENE PLATELETS REINFORCED CORRUGATED WEBS

Yu Wang, Zhan Zhao, Chuang Feng and Jie Yang

School of Engineering, RMIT University
PO BOX 71, Bundoora, VIC 3083 Australia
chuang.feng@rmit.edu.au

Keywords: Eigenvalue buckling; Corrugated webs; Functionally graded material; Graphene platelets

ABSTRACT

Corrugated webs are extensively used in various engineering fields. In this paper, a new novel class of multi-layered corrugated webs reinforced by non-uniformly distributed graphene platelets (GPLs) is proposed. Finite element method (FEM) is employed to investigate the eigenvalue buckling behaviours of the corrugated webs. The effective Young's modulus of the composites is calculated by modified Halpin-Tsai model and the Poisson's ratio and mass density are approximated by rule of mixture. Parametric study is conducted on the effects of several factors, including the number of layers, the wave shapes and the distribution, weight fraction and dimension of GPL, on the buckling behaviours of the corrugated web structures. Corrugated webs with three different wave shapes are considered in present study. It is indicated that circular wave shape is favourable in enhancing the buckling behaviours compared to sinusoidal and triangular wave shapes. The comparisons among the GPL distribution patterns as considered demonstrate that placing more GPL fillers near the surfaces of the structures is preferred to increase the buckling rigidity of the corrugated webs. Moreover, it is found that square GPLs have better reinforcing effects than their counterparts with rectangular shape and increasing the length-to-thickness ratio of GPL is beneficial for the reinforcing effects.

1 INTRODUCTION

Corrugated webs are structures usually corrugated in one direction offering continuous self-stiffening effects for thin plates. This could significant reduce the weight and the cost enhancing the application of the structures in various engineering fields [1-3]. During their service life, corrugated webs are susceptible to various failure modes, among which the most significant one is buckling under compression loading [4, 5]. Numerous research work concentrating on the buckling performances of corrugated webs are carried out experimentally [6] and theoretically [7, 8]. To effectively enhance the structural performances of corrugated webs, different kinds of materials are adopted to manufacture corrugated webs, i.e. aluminium, steel and fibre reinforced laminated composite [7, 9]. Recently, adding graphene and its derivatives, i.e. graphene oxide (GO) and graphene platelets (GPLs), into polymers to produce high-performance composite materials and structures has been attracting interests from academic and industrial communities [10-13].

Delamination is one of the key problems that restrict the application of composite materials. Since they were proposed, functional graded materials (FGMs) were regarded as an effective solution to delamination problem due to the continuous variation of material composition and mechanical properties in certain directions [14, 15], which could remarkably decrease the stress concentration in the interface between two dissimilar material constitutes. Massive efforts have been put to investigate the mechanical properties of functional graded material [16-19]. Recently, incorporating the idea of FGMs and graphene reinforced composites to develop structures with improved mechanical performances has been drawing attention from researchers [12, 13]. However, limited work has been found on the analysis of eigenvalue buckling of corrugated web structures.

In this paper, finite element analysis is carried out to study the eigenvalue buckling behaviours of functionally graded GPL reinforced polymer corrugated webs. The effects of factors, including wave

shape, number of waves and distribution pattern, weight fraction and geometry of GPLs, on the buckling performances of the structures are investigated. Figure 1 shows the geometry of corrugated webs studied. *H* and *W* denote the height and width of corrugated webs, respectively. Three different wave shapes, i.e. circular, sinusoidal and triangular as shown in Figure 2, are considered in the present work.

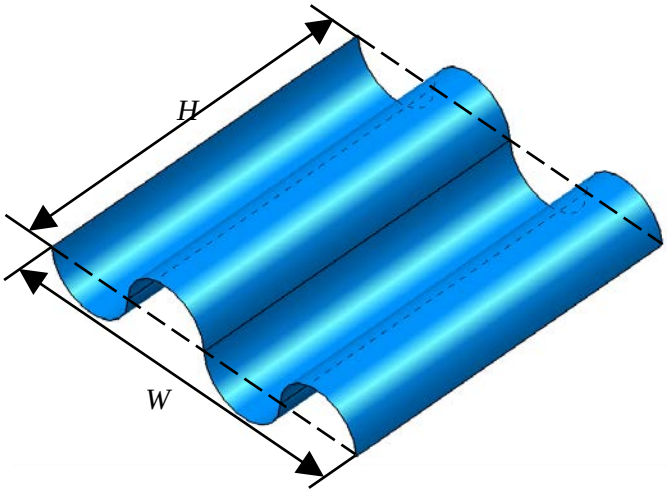

Figure 1 Schematic configuration of corrugated webs

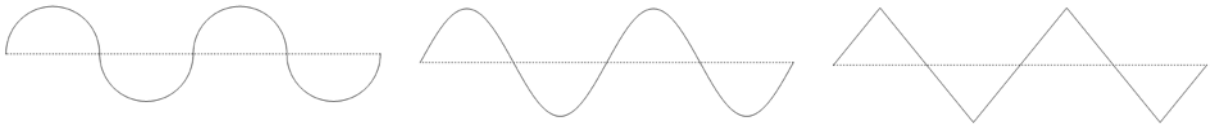

(a) Circular (b) Sinusoidal (c) Triangular

Figure 2 Wave shapes of corrugated web

2 MECHANICAL PROPERTIES OF GPL/POLYMER COMPOSITES

Due to the constraint of current manufacturing technique, the fabrication of FGM structures with GPL concentration varying continuously over thickness direction is very challenging. Alternatively, in this paper, the non-uniform distribution of GPLs along the thickness is realized by stacking up a number of individual layers in the thickness direction. GPLs are uniformly distributed in each individual layer while the GPL concentration varies from layer to layer according to prescribed distribution patterns. For each homogeneous layer, the Young's modulus of the GPL reinforced polymer composites can be estimated as [20]

$$E_{\mathrm{c}} = \frac{3}{8}E_{\parallel} + \frac{5}{8}E_{\perp} \tag{1}$$

where $E_{\parallel}$ and $E_{\perp}$ correspond to the longitudinal and transverse components of the Young's modulus of GPL-Polymer composites, respectively. According to Halpin-Tsai model [21], the two Young's modulus components can be written as

$$E_{\parallel} = \frac{1+\xi_{\mathrm{L}}\eta_{\mathrm{L}}V_{\mathrm{GPL}}}{1-\eta_{\mathrm{L}}V_{\mathrm{GPL}}} \times E_{\mathrm{M}}, \qquad E_{\perp} = \frac{1+\xi_{\mathrm{W}}\eta_{\mathrm{W}}V_{\mathrm{GPL}}}{1-\eta_{\mathrm{W}}V_{\mathrm{GPL}}} \times E_{\mathrm{M}} \tag{2}$$

where E_M and E_{GPL} are the Young's moduli of polymer matrix and the GPL. Given the weight fraction of GPL, i.e. f_{GPL}, and the mass densities of polymer matrix and the GPL, i.e. ρ_M and ρ_{GPL}, the volume fraction of GPL, i.e. V_{GPL}, is approximated as

$$V_{GPL} = \frac{f_{GPL}}{f_{GPL} + (\rho_{GPL}/\rho_M)(1 - f_{GPL})} \tag{3}$$

η_L and η_W in Equation (2) could be expressed as

$$\eta_L = \frac{(E_{GPL}/E_M) - 1}{(E_{GPL}/E_M) + \xi_L}, \quad \eta_W = \frac{(E_{GPL}/E_M) - 1}{(E_{GPL}/E_M) + \xi_W} \tag{4}$$

ξ_L and ξ_W in Equation (4) are parameters characterizing the geometry of reinforcing additives, i.e. graphene platelets, which could be expressed as

$$\xi_L = 2(l_{GPL}/t_{GPL}), \quad \xi_W = 2(w_{GPL}/t_{GPL}) \tag{5}$$

where l_{GPL}, w_{GPL} and t_{GPL} are the average length, width and thickness of the graphene platelets, respectively.

The Young's modulus of GPL/Polymer composite derived by this model could be verified by experimental data as shown in [11]. Apart from Young's modulus, other essential mechanical properties, i.e. Poisson's ratio and mass density of GPL-Polymer composite could be approximated by rule of mixture as

$$\rho_C = \rho_{GPL} V_{GPL} + \rho_M (1 - V_{GPL}) \tag{6}$$

$$\nu_C = \nu_{GPL} V_{GPL} + \nu_M (1 - V_{GPL}) \tag{7}$$

where ν_M and ν_{GPL} are the Poisson's ratio of polymer matrix and graphene platelets, respectively.

2.2 DISTRIBUTION PATTERNS OF GRAPHENE PLATELETS

For the functionally graded corrugated webs, GPLs are non-uniformly distributed along the thickness direction and four distribution patterns are considered in present work. Figure 3 shows the variation of GPL weight fraction in the thickness direction of the corrugated webs. f_{GPL} in Figure 3 denotes the average GPL weight fraction, which is kept the same for all the distribution patterns. t and f represent specified location and the corresponding GPL weight fraction in the thickness direction, respectively. For pattern 1, the GPL weight fraction is a constant along the thickness of the webs, which means GPLs are dispersed uniformly in the polymer. The GPL weight fraction grows linearly from 0 in the bottom and top surfaces to $2f_{GPL}$ in the mid-plane for Pattern 2. In contrast, pattern 3 has the greatest GPL weight fraction on the two surfaces and smallest GPL weight fraction in the mid-plane. For pattern 4, the weight fraction increases linearly from 0 to $2f_{GPL}$ between two surfaces.

As mentioned, it is very challenging to implement smooth variation of GPL weight fraction along the thickness direction due to constraint of current manufacturing technique. The corrugated webs here are consisting of a number of layers, i.e. N = 4, 6, 8, 10, to approximate FGM structures. The weight fraction of GPL remains constant in each individual layer. As an example, Table 1 illustrates the distribution of weight fraction of GPLs in the thickness direction for 10-layered corrugated webs with average weight fraction being 0.5%

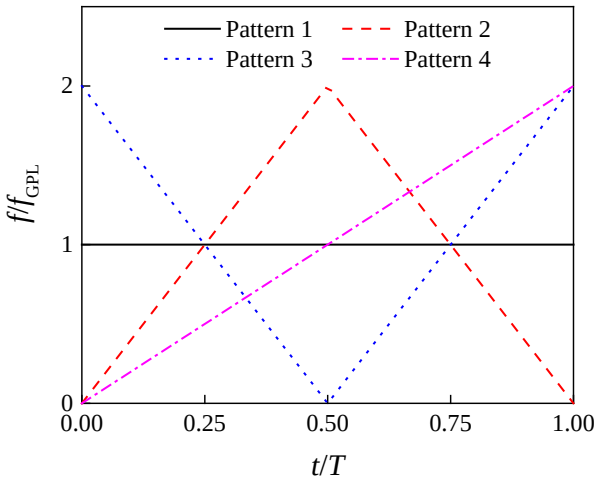

Figure 3 GPL weight fraction in the thickness direction of corrugated webs

Table 1 Weight fraction of GPLs for 10-layered corrugated webs (f_{GPL} = 0.5%)

Layer No.	Pattern 1	Pattern 2	Pattern 3	Pattern 4
1	0.500%	0.000%	1.000%	0.000%
2	0.500%	0.250%	0.750%	0.111%
3	0.500%	0.500%	0.500%	0.222%
4	0.500%	0.750%	0.250%	0.333%
5	0.500%	1.000%	0.000%	0.444%
6	0.500%	1.000%	0.000%	0.556%
7	0.500%	0.750%	0.250%	0.667%
8	0.500%	0.500%	0.500%	0.778%
9	0.500%	0.250%	0.750%	0.889%
10	0.500%	0.000%	1.000%	1.000%

2.3 FINITE ELEMENTM ANALYSIS MODELLING

Slender and thin structures are susceptible to buckling failure. Eigenvalue buckling analysis aims to predict the critical buckling load and failure mode of a structure with no imperfections. For eigenvalue buckling analysis, the problem can be described by the following governing equation

$$K^{MN} q^{M} = 0 \tag{8}$$

where K^{MN} and q^{M} in Equation (8) corresponds to tangent stiffness matrix and displacement vector, respectively. When the applied buckling load reaches a critical value, the above governing equation will have non-trivial solution, i.e. $q^{M} \neq 0$. Therefore, the eigenvalue buckling analysis is to identify the critical buckling load that enables Equation (8) to have non-trivial solution.

Finite element package ABAQUS is used here to carry out eigenvalue buckling analysis for the corrugated web in present work. The boundary conditions and loads are shown in Figure 4. The displacement in x direction and y direction together with the rotation of edge AB and edge CD are fully constrained. The edge AC and edge BD are free. Shell edge load is applied in edge AB and edge CD. Shell element S4R is adopted for the finite element model. Subspace eigensolver in ABQUS/Standard is used to extract eigenvalue and eigenvector.

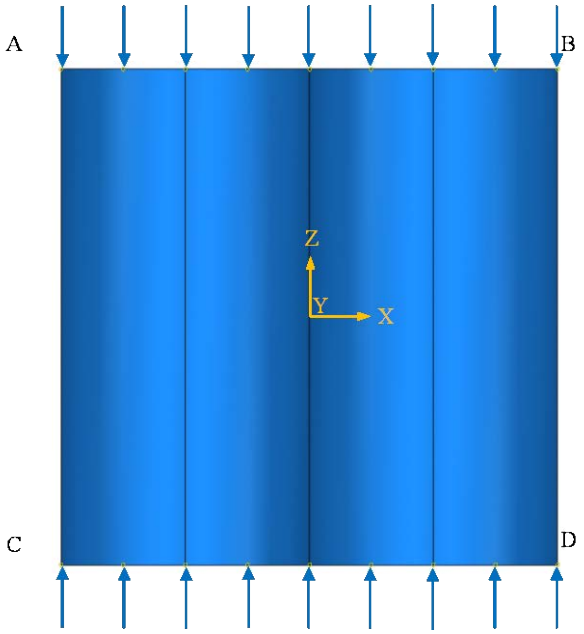

Figure 4 Boundary conditions and loads

3 RESULTS AND DISCUSSION

3.1 VALIDATION OF FINITE ELEMENT MODEL

The finite element analysis in present study is validated by comparing the critical buckling stress for a homogenous flat plate. The height, width and thickness of the homogenous plate are 100 mm, 100 mm and 1 mm, respectively. Epoxy is selected as the polymer matrix. The material properties of the GPL and the epoxy are listed in Table 2. The average length, width and thickness of graphene platelets are 2.5 μm, 1.5 μm and 1.5 nm, respectively. The height, width and thickness of corrugated webs are 100 mm, 100 mm and 4 mm, respectively. The material of the plate is selected as pure epoxy, whose material properties are shown in Table 2. According to Ref. [22], the critical buckling stress of a homogenous flat plate subjected to uni-axial compression can be estimated as

$$\sigma_{cr} = \frac{k\pi^2 E}{12\left(1-\nu^2\right)\left(b/t\right)^2} \tag{9}$$

where E and v are the Young's modulus and Poisson's ratio of the material, b and t are the width and thickness of the plate. k is the plate buckling coefficient, which is related to load condition and boundary condition. In the present study, k = 4 [22]. The critical buckling stress calculated by Equation (9) is 1.116 MPa while the result derived by present finite element analysis is 1.082 MPa. The relative error between the finite element result and theoretical result is 3.1%.

Table 2 Material properties of graphene platelets and epoxy

	GPL	Epoxy
Young's modulus (GPa)	1010	2.85
Poisson's ratio	0.2	0.38
Mass density (g/cm^3)	1.06	1.2

3.2 PARAMETRIC STUDY

The effect of the number of layers is presented in Figure 5, in which corrugated webs with 6 sinusoidal waves and 0.5% weight fraction of GPLs are considered. The results suggest that number of layers has very limited effects on the critical buckling stress of the web structures with distribution patterns 1, 3 and 4. However, it can be seen that the buckling stress increases as the number of layers increases for pattern 2. The comparisons in this figure advise that among the four distribution patterns as considered, pattern 3 is the most favorable GPL distribution in enhancing the buckling performances of the corrugated webs. Figure 6 plots the influences of the number of waves and wave shape on the critical buckling stress for corrugated webs with distribution pattern 1 and 0.5% weight fraction of GPL. Apparently, the critical buckling stress grows dramatically when the wave number increases from 1 while it drops sharply when the number of waves is greater than a critical value. This indicates that there exist optimal numbers of waves for each shape, which enable the structures to have the largest buckling stress. The result also shows circular wave shape has the best reinforcing effect when the wave number is approximately smaller than 6. When the wave number exceeds 7, sinusoidal wave has better reinforcing effect compared to the other two wave shapes, i.e. circular and triangular.

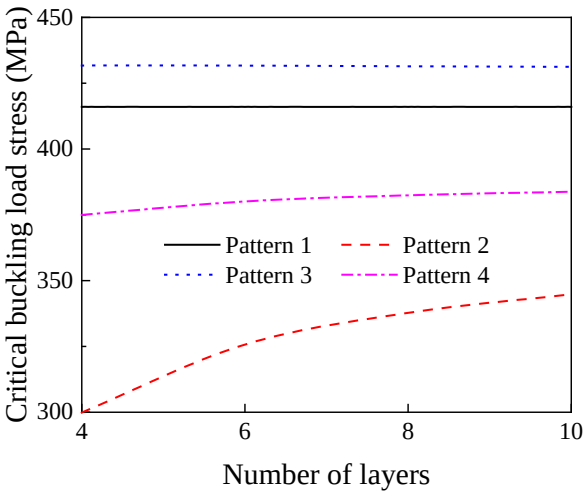

Figure 5 Effect of number of layers on critical buckling stress

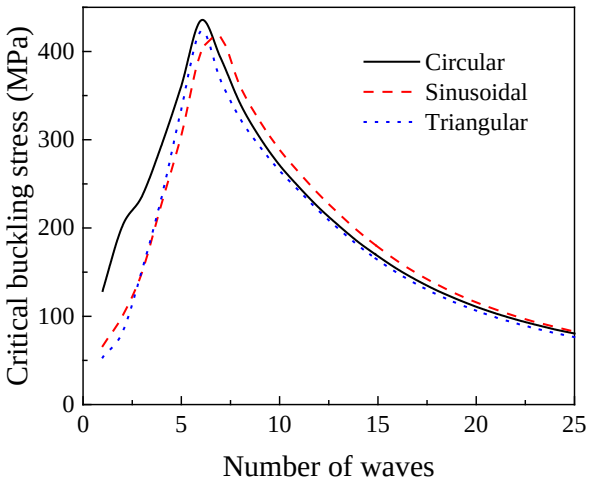

Figure 6 Effect of wave number and shapes on critical buckling stress

Figure 7 presents the variation of the critical buckling stress of corrugated webs with the average GPL weight fraction. The corrugated webs have 6 sinusoidal waves. It can be seen that the buckling

stress can be significantly enhanced by adding a very small amount of GPL as reinforcing fillers. In addition, the buckling stress is more sensitive to GPL weight fraction for corrugated webs with distribution 3 compared to the other three patterns. The geometry of GPLs has significant impacts on the reinforcing effects, thereby affects the buckling behaviours of corrugated webs. Figure 8 investigates the effects of GPL dimension, i.e. length-to-thickness ratio *l/t*, on the critical buckling stress. The result demonstrates that the increase of the GPL length-to-thickness ratio greatly improves the buckling performances when the ratio is within a certain range, i.e. $100 \leq l/t \leq 1000$ and the increasing rate drops down as this ratio further increase. In addition, the comparison between the curves indicates that GPLs with smaller aspect ratio, i.e. *l/w*, are better reinforcing fillers than their counterparts with smaller aspect ratio. The above phenomena can be explained by the fact that GPLs with larger length-to-thickness ratio and smaller aspect ratio have larger surface areas, resulting in better bonding and load transfer between the polymer matrix and the fillers.

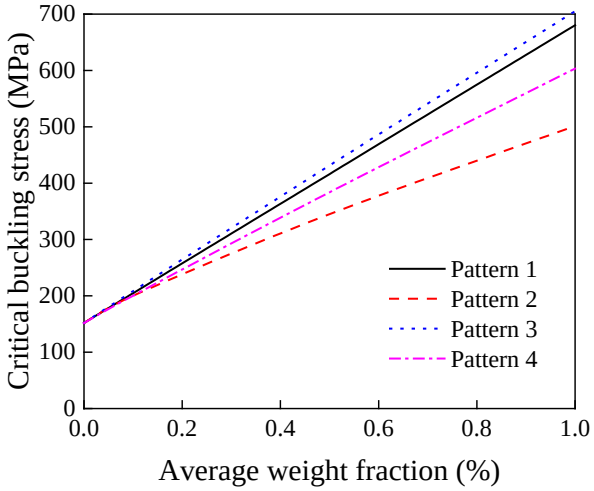

Figure 7 Effect of GPL weight fraction and distribution pattern on critical buckling stress

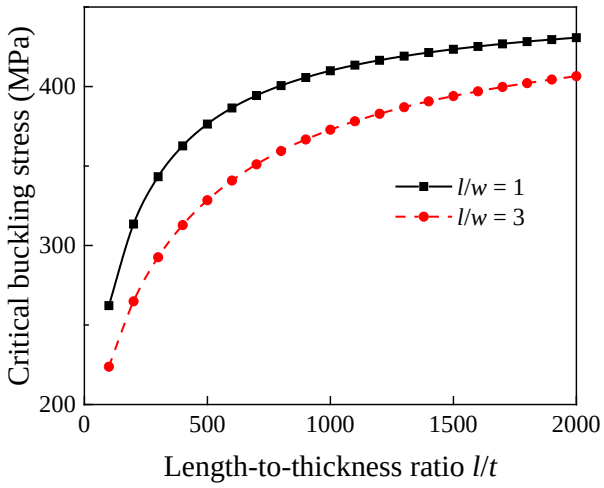

Figure 8 Effect of GPLs geometry on critical buckling stress

4 CONCLUSIONS

The eigenvalue buckling behaviours of functionally graded GPL reinforced corrugated webs are investigated by finite element analysis. Parametric study is conducted to investigate the effects of number of layers, wave shape, GPL distribution pattern and dimensions on the buckling performances

of the corrugated web structures. The results reveal that in addition to weight fraction GPL distribution has significant effects on the buckling stress of the corrugated webs. Pattern 3 is found to be the most favorable way to improve the buckling behaviours of the structures. The number of waves also has considerable effects on the buckling and there exist critical numbers of waves that could enable the structures to sustain the greatest buckling load. Moreover, the study on effects of the GPL dimension suggests that GPLs with larger surface area and fewer graphene layers are preferred in enhancing the buckling performances of the web structures.

ACKNOWLEDGEMENTS

The work described in this paper is fully funded by a research grant from the Australian Research Council under Discovery Early Career Researcher Award (DECRA) scheme (DE160100086). The authors are grateful for the financial support from the Australian Research Council under Discovery Project scheme (DP160101978).

REFERENCES

[1] M. Bahrebar, M.Z. Kabir, T. Zirakian, M. Hajsadeghi, J.B.P. Lim, Structural performance assessment of trapezoidally-corrugated and centrally-perforated steel plate shear walls, Journal of Constructional Steel Research 122 (2016) 584-594.
[2] E.Y. Sayed-Ahmed, Design aspects of steel I-girders with corrugated steel webs, Lateral (2001) 2005a.
[3] H.-H. Sun, J. Spencer, Buckling strength assessment of corrugated panels in offshore structures, Marine Structures 18(7–8) (2005) 548-565.
[4] R. Luo, B. Edlund, Buckling analysis of trapezoidally corrugated panels using spline finite strip method, Thin-Walled Structures 18(3) (1994) 209-224.
[5] M. Malinowski, T. Belica, K. Magnucki, Buckling and post-buckling behaviour of elastic seven-layered cylindrical shells – FEM study, Thin-Walled Structures 94 (2015) 478-484.
[6] B. Jáger, L. Dunai, B. Kövesdi, Experimental investigation of the M-V-F interaction behavior of girders with trapezoidally corrugated web, Engineering Structures 133 (2017) 49-58.
[7] J. Viguié, P.J.J. Dumont, Analytical post-buckling model of corrugated board panels using digital image correlation measurements, Composite Structures 101 (2013) 243-254.
[8] K.M. Liew, L.X. Peng, S. Kitipornchai, Buckling analysis of corrugated plates using a mesh-free Galerkin method based on the first-order shear deformation theory, Computational Mechanics 38(1) (2006) 61-75.
[9] E.Y. Sayed-Ahmed, Behaviour of steel and (or) composite girders with corrugated steel webs, Canadian Journal of Civil Engineering 28(4) (2001) 656-672.
[10] C. Lee, X. Wei, J.W. Kysar, J. Hone, Measurement of the Elastic Properties and Intrinsic Strength of Monolayer Graphene, Science 321(5887) (2008) 385.
[11] M.A. Rafiee, J. Rafiee, Z. Wang, H. Song, Z.Z. Yu, N. Koratkar, Enhanced mechanical properties of nanocomposites at low graphene content, ACS Nano 3(12) (2009) 3884-3890.
[12] C. Feng, S. Kitipornchai, J. Yang, Nonlinear free vibration of functionally graded polymer composite beams reinforced with graphene nanoplatelets (GPLs), Engineering Structures 140 (2017) 110-119.
[13] C. Feng, S. Kitipornchai, J. Yang, Nonlinear bending of polymer nanocomposite beams reinforced with non-uniformly distributed graphene platelets (GPLs), Composites Part B: Engineering 110 (2017) 132-140.
[14] D.K. Jha, T. Kant, R.K. Singh, A critical review of recent research on functionally graded plates, Composite Structures 96 (2013) 833-849.
[15] S. Suresh, A. Mortensen, Fundamentals of functionally graded materials, The Institut of Materials1998.

[16] K.M. Liew, Z.X. Lei, L.W. Zhang, Mechanical analysis of functionally graded carbon nanotube reinforced composites: A review, Composite Structures 120 (2015) 90-97.
[17] E. García-Macías, L. Rodriguez-Tembleque, R. Castro-Triguero, A. Sáez, Buckling analysis of functionally graded carbon nanotube-reinforced curved panels under axial compression and shear, Composites Part B: Engineering 108 (2017) 243-256.
[18] J. Yang, L.-L. Ke, C. Feng, Dynamic buckling of thermo-electro-mechanically loaded FG-CNTRC beams, International Journal of Structural Stability and Dynamics 15(08) (2015) 1540017.
[19] J. Yang, S. Kitipornchai, C. Feng, Nonlinear vibration of PZT4/PZT-5H monomorph and bimorph beams with graded microstructures, International Journal of Structural Stability and Dynamics 15(07) (2015) 1540015.
[20] R.G.d. Villoria, A. Miravete, Mechanical model to evaluate the effect of the dispersion in nanocomposites, Acta Materialia 55(9) (2007) 3025-3031.
[21] J.C.H. Affdl, J.L. Kardos, The Halpin-Tsai equations: a review, Polymer Engineering & Science 16(5) (1976) 344-352.
[22] P.S. Bulson, The stability of flat plates, Elsevier Publishing Company1969.